Electronic Supplementary Information (ESI)

Ground-State Intramolecular Proton-Transfer Inhibits the Selective Methylation on Quinoline and Pyridine Derivatives

Supphachok Chanmungkalakul,[‡a] Shiqing Huang,[‡a,b] Xia Wu,[a] Esther Cai Xia Ang,[c] Zi-Qi Yang,[c] Yongxin Li,[c] Xiaoyu Yan,[b] Choon-Hong Tan,[c] Davin Tan,[a]* and Xiaogang Liu[a]*

[a]*Fluorescence Research Group, Singapore University of Technology and Design, 8 Somapah Road, 487372 Singapore, Singapore*

[b]*Department of Chemistry, Renmin University of China, 100872 Beijing, China*

[c]*School of Chemistry, Chemical Engineering and Biotechnology, Nanyang Technological University, 637459 Singapore, Singapore*

‡These authors contributed equally.

Email: davin_tan@mail.mcgill.ca (D. T.); xiaogang_liu@sutd.edu.sg (X. L.)

Table of Contents

List of Figures

List of Tables

1. Chemicals and instruments

All of the chemicals were purchased from Sigma Aldrich and Tokyo Chemical Industry (TCI) and used without further purification.

^{1}H NMR spectra were collected using Bruker AV-300 (300 MHz), and Bruker Avance III 400 (400MHz) spectrometer. The NMR spectra were plotted using the academic version of Topspin™. Chemical shifts are recorded as δ in units of parts per million (ppm). HPLC analysis was conducted on Shimadzu LC-20AT and LC-2010CHT HPLC workstations. High-resolution mass spectra (HRMS) were obtained by Q-Tof Premier mass spectrometer (Waters Corporation).

2. Computational methods

The geometry optimizations of ground and transition states were performed with *Gaussian 16*.[1] All calculations were carried out with M062X/Def2SVP level of theory. The solvent effects (in ethyl acetate) were accounted for using the SMD model.[2]

3. General reactions

All the reactions were carried out via the same procedure unless stated otherwise. 1 mmol of N-heterocyclic precursor molecules was added into 3 mL of EA in a 5 mL vial with a stirrer bar. Subsequently, 3 mmol of MeI was added to the solution. The resulting solution was stirred for 3 to 6 hours at room temperature. The precipitate would start to form several minutes after adding MeI. The precipitate was filtered and washed with EA several times. The products were obtained in brownish orange solid. This reaction could be upscaled to a gram scale with 10 mmol of starting materials. For alkylating reagents, methyl iodide and ethyl iodide were used while propyl bromide and butyl bromide were used.

4. Molecule characterizations

4-amino-2-methylisoquinolin-2-ium iodide (1)

Yield: 98.9% in the mmol scale (94.1% in the gram scale). ^{1}H NMR (400 MHz, DMSO-*d6*) *δ* (ppm): 4.317 (CH_3 of N-methyl), 7.224 and 7.706 (NH_2 of amino), 7.706-8.994 (H of aromatic ring) as shown in Fig S8. $^{13}C\{^1H\}$ NMR (400 MHz, DMSO-*d6*) *δ* (ppm): 47.849 (CH_3 of N-methyl), 117.010-143.499 (C of aromatic ring) as shown in Fig S9. HRMS (ESI): $C_{10}H_{11}N_2^+$, calcd m/z : 159.0922, found m/z: 159.0920.

4-amino-2-ethylisoquinolin-2-ium iodide (2)

Yield: 73.7% in the mmol scale. ^{1}H NMR (400 MHz, D_2O) *δ* (ppm): 1.458-1.495 (CH_3 of N-methyl), 4.248-4.303 (CH_2 of N-methyl), 7.246-7.692 (H of aromatic ring), 8.004 and 8.349 (NH_2 of amino) as shown in Fig S10. $^{13}C\{^1H\}$ NMR (400 MHz, D_2O) *δ* (ppm): 15.556 (CH_3 of N-methyl), 56.787 (CH_2 of N-methyl), 115.984-141.779 (C of aromatic ring) as shown in Fig S11. HRMS (ESI): $C_1{}^1H_{13}N_2^+$, calcd m/z : 173.1079, found m/z: 173.1075.

4-amino-2-propylisoquinolin-2-ium bromide (3)

Yield: 65.3% in the mmol scale. ^{1}H NMR (400 MHz, D_2O) *δ* (ppm): 0.924-0.954 (CH_3 of N-methyl), 1.978-1.995 (CH_2 of N-methyl), 4.369-4.382 (CH_2 of N-methyl), 7.550-7.881 (H of aromatic ring), 8.553 (NH_2 of amino) as shown in Fig S12. $^{13}C\{^1H\}$ NMR (400 MHz, D_2O) *δ* (ppm): 9.837 (CH_3 of N-methyl), 24.014 (CH_2 of N-methyl), 62.980 (CH_2 of N-methyl), 116.305-143.788 (C of aromatic ring) as shown in Fig S13. HRMS (ESI): $C_{12}H_{15}N_2^+$, calcd m/z : 187.1235, found m/z: 187.1221.

4-amino-2-buthylisoquinolin-2-ium bromide (4)

Yield: 87.3% in the mmol scale. ^{1}H NMR (400 MHz, D_2O) δ (ppm): 0.938-0.975 (CH_3 of N-methyl), 1.311-1.404 (CH_2 of N-methyl), 1.942-2.016 (CH_2 of N-methyl), 4.445-4.482 (CH_2 of N-methyl), 7.666-8.019 (H of aromatic ring), 8.685 (NH_2 of amino) as shown in Fig S14. $^{13}C\{^{1}H\}$ NMR (400 MHz, D_2O) δ (ppm): 12.669 (CH_3 of N-methyl), 18.790 (CH_2 of N-methyl), 65.369 (CH_2 of N-methyl), 61.390 (CH_2 of N-methyl), 116.635-143.932 (C of aromatic ring) as shown in Fig S15. HRMS (ESI): $C_{13}H_{17}N_2^+$, calcd m/z : 201.1392, found m/z: 201.1384.

6-amino-1-methylquinolin-1-ium iodide (5)

Yield: 72.0 %. ^{1}H NMR (400 MHz, MeOH-*d4*) δ (ppm): 4.558 (CH_3 of N-methyl), 7.208-7.215 (NH_2 of amino), 7.657-8.878 (H of aromatic ring) as shown in Fig S16. $^{13}C\{^{1}H\}$ NMR (400 MHz, MeOH-*d4*) δ (ppm): 44.611 (CH_3 of N-methyl), 105.844-150.292 (C of aromatic ring) as shown in Fig S17. HRMS (ESI): $C_{10}H_{11}N_2^+$, calcd m/z : 159.0922, found m/z: 159.0928.

6-amino-1-buthylquinolin-1-ium bromide (6)

Yield: 9.2%. ^{1}H NMR (400 MHz, $CHCl_3$-d) δ (ppm): 0.825-0.906, (CH_2 of N-methyl), 0.965-1.002 (CH_3 of N-methyl), 1.446-1.503 (CH_2 of N-methyl), 1.638-1.711 (CH_2 of N-methyl), 3.189-3.225 (NH_2 of amino), 6.672-8.590 (H of aromatic ring) as shown in Fig S18. $^{13}C\{^{1}H\}$ NMR (400 MHz, $CHCl_3$-d) δ (ppm): 13.904-43.631 (alkyl group of N-methyl), 102.572-146.518 (C of aromatic ring) as shown in Fig S19, noted that this NMR spectrum contains a small amount Ethyl Acetate. HRMS (ESI): $C_{13}H_{17}N_2^+$, calcd m/z : 201.1392, found m/z: 201.1390.

1-methylpyrazin-1-ium iodide (7)

Yield: 97.1%. ^{1}H NMR (400 MHz, DMSO-*d6*) δ (ppm): 4.566 (CH_3 of N-methyl), 9.054, and 9.491 (H of aromatic ring) as shown in Fig S20. $^{13}C\{^{1}H\}$ NMR (400 MHz, DMSO-*d6*) δ (ppm): 137.750-150.612 (C of aromatic ring) as shown in Fig S21, noted that the structure was also confirmed by the crystal structure. HRMS (ESI): $C_5H_7N_2^+$, calcd m/z : 95.0609, found m/z: 95.0608.

5-amino-2-bromo-1-methylpyrazin-1-ium iodide (8)

Yield: 56.0%. ^{1}H NMR (400 MHz, DMSO-*d6*) δ (ppm): 3.740 (CH_3 of N-methyl), 8.098, and 8.382 (H of aromatic ring) as shown in Fig S22. $^{13}C\{^{1}H\}$ NMR (400 MHz, DMSO-*d6*) δ (ppm): 41.376 (CH_3 of N-methyl), 121.208-141.843 (C of aromatic ring) as shown in Fig S23. HRMS (ESI): $C_5H_7BrN_3^+$, calcd m/z : 187.9823, found m/z: 187.9817.

3-amino-1-methylpyridin-1-ium iodide (9)

Yield: 94.0%. ^{1}H NMR (400 MHz, DMSO-*d6*) δ (ppm): 4.179 (CH_3 of N-methyl), 6.586 (NH_2 of amino), 7.554-8.056 (H of aromatic ring) as shown in Fig S24. $^{13}C\{^{1}H\}$ NMR (400 MHz, DMSO-*d6*) δ (ppm): 48.346 (CH_3 of N-methyl), 127.291-148.626 (C of aromatic ring) as shown in Fig S25. HRMS (ESI): $C_5H_7BrN_3^+$, calcd m/z : 109.0766, found m/z: 109.0768.

3-hydroxy-2-iodo-1-methylpyridin-1-ium iodide (10)

Yield: 89.8%. ^{1}H NMR (400 MHz, DMSO-*d6*) δ (ppm): broad peak at 3.678 (proton transferred species of -OH of aromatic ring),4.406 (CH_3 of N-methyl), 7.682-7.813 (H of aromatic ring), 8.750 and 8.764 (NH_2 of amino), as shown in Fig S26. $^{13}C\{^{1}H\}$ NMR (400 MHz, DMSO-*d6*) δ (ppm): 56.030 (CH_3 of N-methyl), 117.258-159.607 (C of aromatic ring) as shown in Fig S27. HRMS (ESI): $C_6H_7INO^+$, calcd m/z : 235.9572, found m/z: 235.9565.

3-carboxy-1-methylpyridin-1-ium iodide (11)

Yield: 42.0%. ^{1}H NMR (400 MHz, DMSO-*d6*) δ (ppm): broad peak at 3.990 (proton transferred species of -COOH of aromatic ring), 4.417 (CH_3 of N-methyl), 8.207-9.468 (H of the aromatic ring as shown in Fig S28. ^{13}C{^{1}H} NMR (400 MHz, DMSO-*d6*) δ (ppm): 48.713 (CH_3 of N-methyl), 128.275-148.831 (C of aromatic ring), 163.584 (-COOH of aromatic ring), as shown in Fig S29. HRMS (ESI): $C_7H_8NO_2^+$, calcd m/z : 138.0555, found m/z: 138.0558.

3-methylbenzo[d]thiazol-3-ium iodide (12)

Yield: 21.2 %. ^{1}H NMR (400 MHz, DMSO-*d6*) δ (ppm): 4.396 (CH_3 of N-methyl), 7.841-8.516, and 10.516 (H of aromatic ring) as shown in Fig S30. ^{13}C{^{1}H} NMR (400 MHz, DMSO-*d6*) δ (ppm): 117.599-131.574 and 165.302 (C of aromatic ring), 163.584 (-COOH of aromatic ring), as shown in Fig S31. HRMS (ESI): $C_8H_8NS^+$, calcd m/z : 150.0377, found m/z: 150.0380.

2-(methylthio)pyridine (13'')

Yield: 99.1%. ^{1}H NMR (400 MHz, DMSO-*d6*) δ (ppm): 2.654 (S-CH_3), 7.443-8.582 (H of aromatic ring) as shown in Fig S32. ^{13}C{^{1}H} NMR (400 MHz, DMSO-*d6*) δ (ppm): 14.214 (S-CH_3), 121.431-158.682 (C of aromatic ring), as shown in Fig S33, noted that the structure was also confirmed by the crystal structure.

Table S1. General and X-ray crystallographic data for obtainable products

Name	**1**	**3**	**5**
Molecular Formula	$C_{10}H_{11}IN_2$	$C_{12}H_{15.25}BrN_2O_{0.125}$	$C_{10}H_{13}IN_2O$
M_r	286.11	269.42	304.12
Crystal System	orthorhombic	monoclinic	monoclinic
Space group	*F*ddd	$P2_1/c$	P121/c1
Unit cell dimensions (Å,°)			
a	6.7210(3)	15.3346(6)	7.3757(6)
b	19.9988(11)	15.1704(6)	19.8901(17)
c	32.6212(19)	10.1934(5)	8.6493(7)
α	90	90	90
β	90	91.8457(16)	114.402(3)
γ	90	90	90
Volume ($Å_3$)	4384.7(4)	2370.08(18)	1155.53(17)
Z	16	8	4
Temperature (K)	100.(2)	100.(2)	100.(2)
Crystal Colour	yellow	yellow	orange
D_{calc} (g cm^{-3})	1.734	1.51	1.748
F(000)	2208	1098	592
μ (mm^{-1})	2.88	3.44	2.743
R [*gt*]	0.0965	0.0467	0.0323
Goodness-of-fit on F^2	1.138	1.016	1.048
CCDC code	2128396	2128397	2142749

Name	**7**	**8**	**10**
Molecular Formula	$C_5H_5IN_2$	$C_5H_7I_2N_3$	$C_{12}H_{13}I_3N_2O_2$
Mr	220.01	362.94	597.94
Crystal System	tetragonal	hexagonal	orthorhombic
Space group	*I*4/mmm	$P6_1$	$P2_12_12_1$
Unit cell dimensions (Å,°)			
a	10.3872(3)	7.0916(2)	8.2027(3)
b	10.3872(3)	7.0916(2)	13.5124(4)
c	13.2209(6)	31.4164(13)	14.3668(5)
α	90	90	90
β	90	90	90
γ	90	120	90
Volume ($Å^3$)	1426.45(10)	1368.28(10)	1592.39(9)
Z	8	6	4
Temperature (K)	100.(2)	100.(2)	100.(2)
Crystal Colour	yellow	yellow	yellow
Dcalc (g cm^{-3})	2.049	2.643	2.494
F(000)	816	984	1096
μ (mm^{-1})	4.391	6.832	5.888
R [*gt*]	0.0359	0.0397	0.039
Goodness-of-fit on F^2	1.021	1.033	0.994
CCDC code	2128398	2128399	2128400

Name	**13''**
Molecular Formula	C_6H_8INS
Mr	253.09
Crystal System	monoclinic
Space group	$P2_1/c$
Unit cell dimensions (Å,°)	
a	6.9824(9)
b	15.4554(19)
c	7.8105(11)
α	90
β	91.042(7)
γ	90
Volume (Å^3)	842.74(19)
Z	4
Temperature (K)	100.(2)
Crystal Colour	yellow
Dcalc (g cm^{-3})	1.995
F(000)	480
μ (mm^{-1})	3.966
R [*gt*]	0.0415
Goodness-of-fit on F^2	0.978
CCDC code	2128401

*$R = \Sigma||F_o|-|F_c||/\Sigma Fo, w = 1/[\sigma_2(F_o^2)+(g_1P)^2+ g2P]$ where P = (Fo2+2Fc2)/3, $S = \Sigma[w(Fo2 – Fc2)2/(Nobs – Nparam)]^{1/2}$.

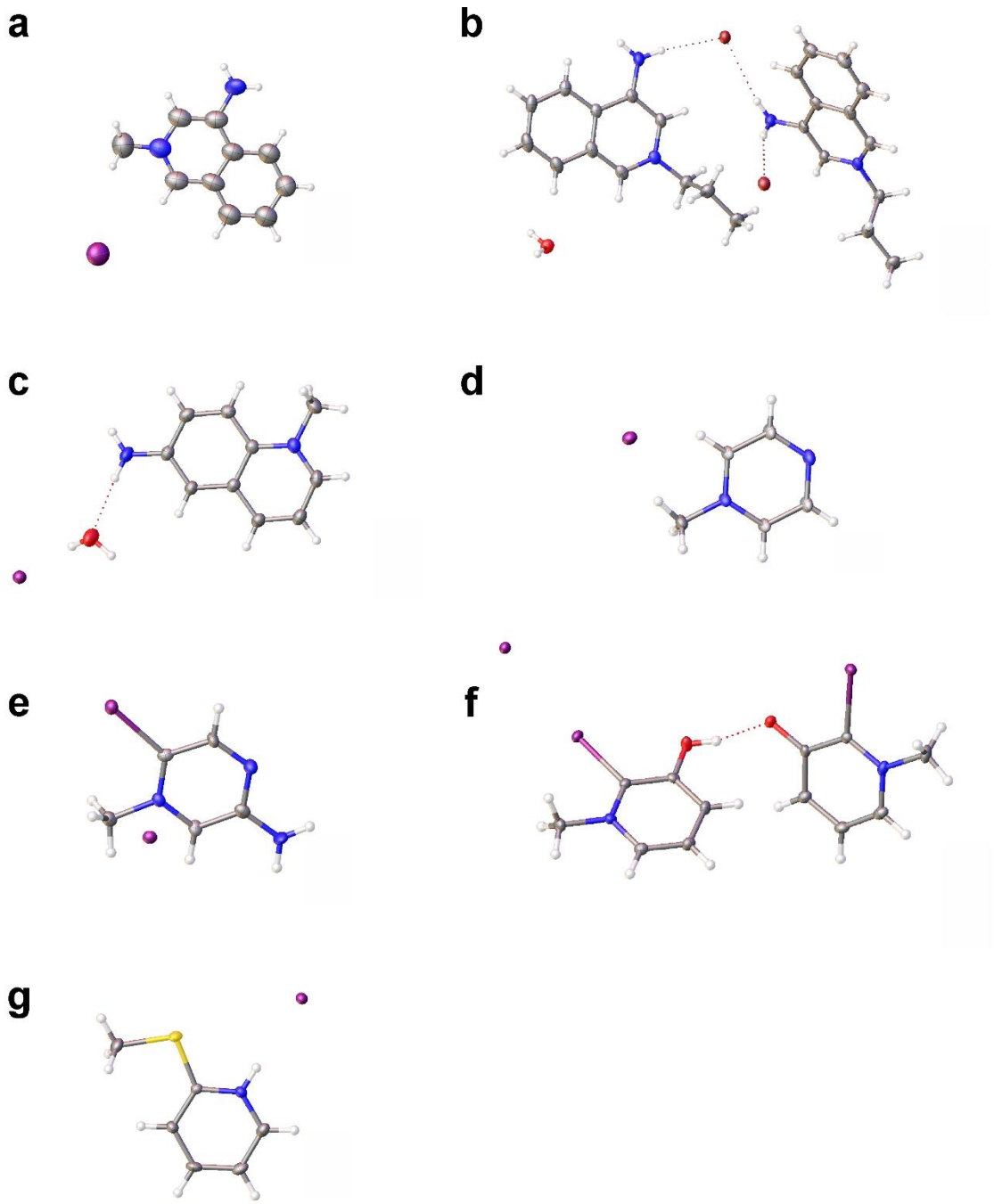

Figure S1. The asymmetric units in the crystal structures of (a) **1**, (b) **3**, (c) **5**, (d) **7**, (e) **8**, (f) **10,** and (g) **13''**.

5. The Gibbs free energy of N-alkylated and alkylated products in comparison to their starting materials

Table S2. The Gibbs free energy of N-alkylated and alkylated products in comparison to their starting materials

Product name	Total Gibbs free energy of starting materials (kcal/mol)	Total Gibbs free energy of products (kcal/mol)	ΔG (kcal/mol)
2	-522928.83	-522940.74	-11.91
2'	-522928.83	-522926.78	2.05
3	-547550.64	-547560.97	-10.33
3'	-547550.64	-547548.74	1.90
4	-572172.29	-572183.73	-11.44
4'	-572172.29	-572170.36	1.93
5	-498307.81	-498316.45	-8.63
5'	-498307.81	-498306.00	1.81
6	-572174.42	-572181.46	-7.04
6'	-572174.42	-572172.01	2.42

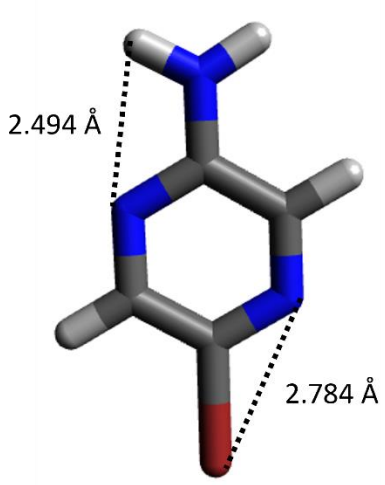

Figure S2. Optimized geometry of the starting material to form **8**. The inset shows the distances between the N atoms to their neighboring substituents (including -NH_2 and -Br).

6. Full IRC calculations of transition states

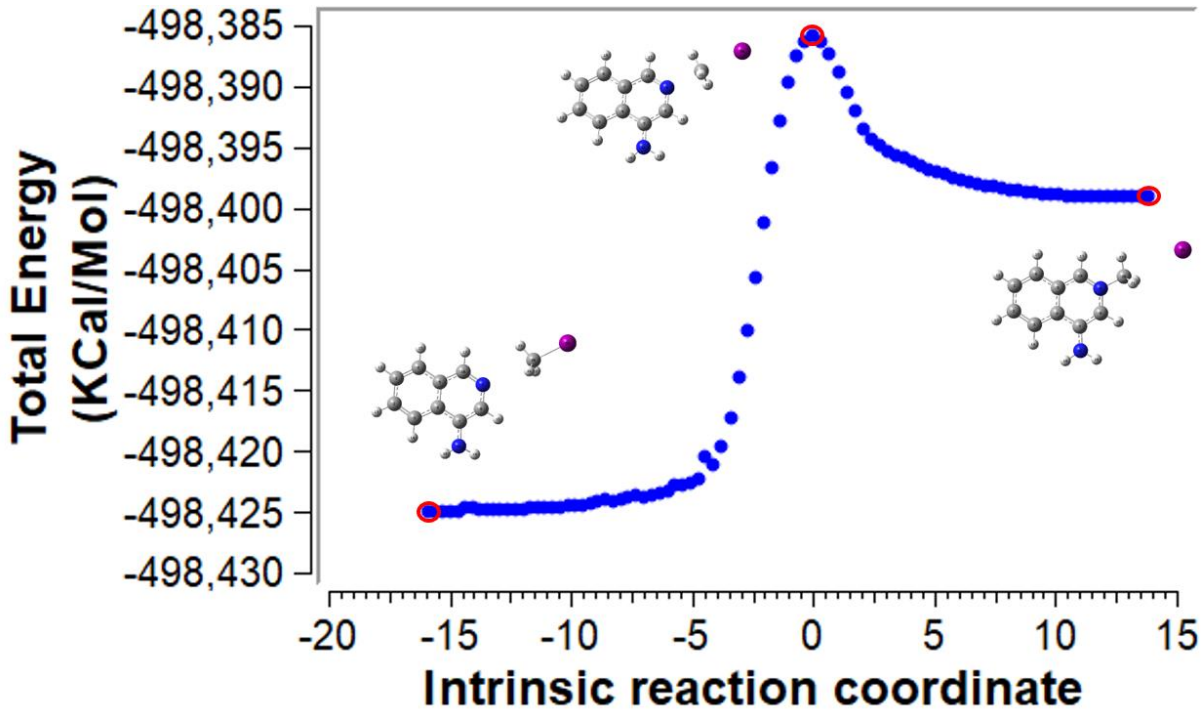

Figure S3. Full IRC calculations from the transition state of **1**.

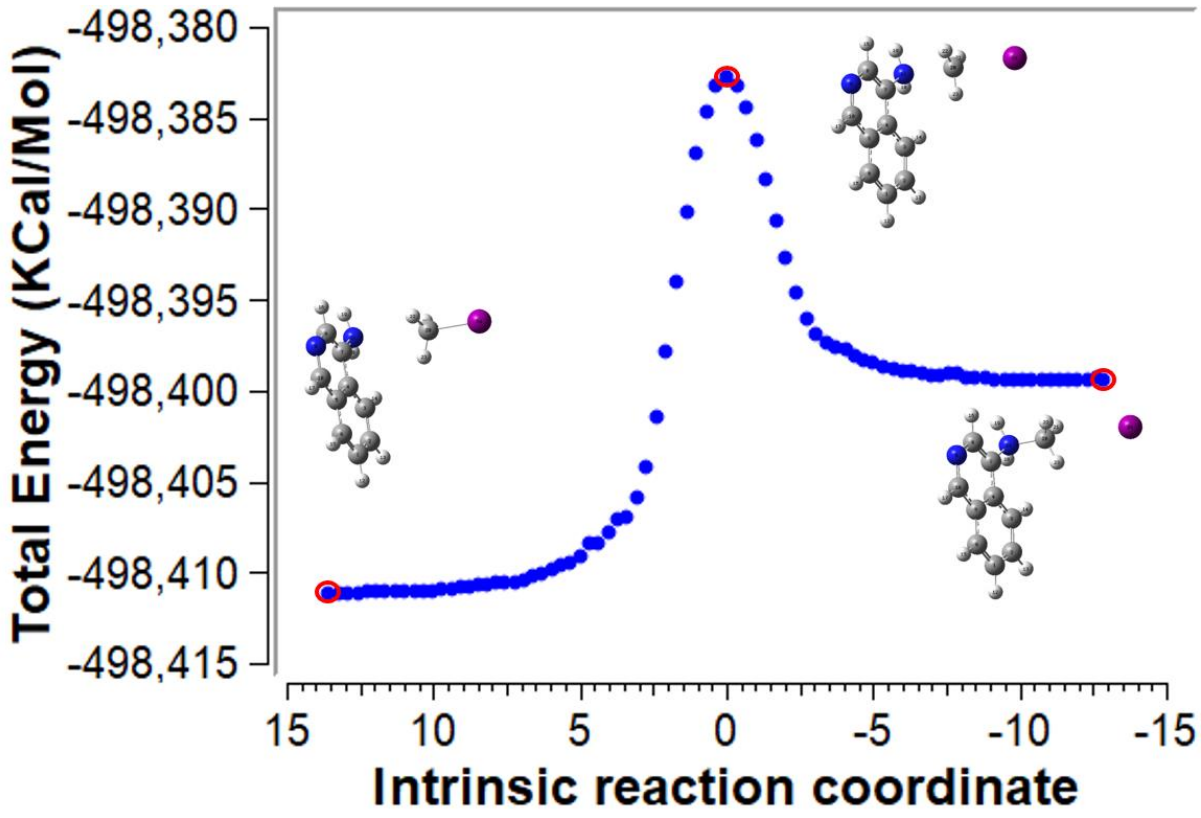

Figure S4. Full IRC calculations from the transition state of **1'**.

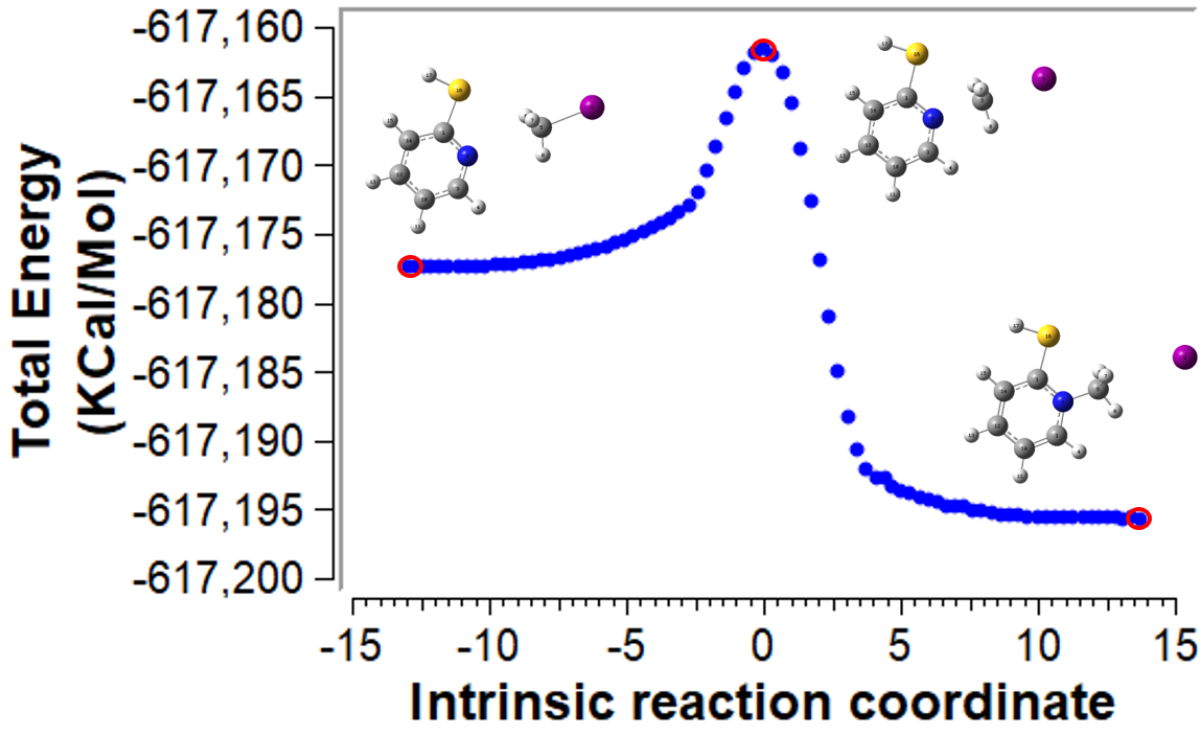

Figure S5. Full IRC calculations from the transition state of **13**.

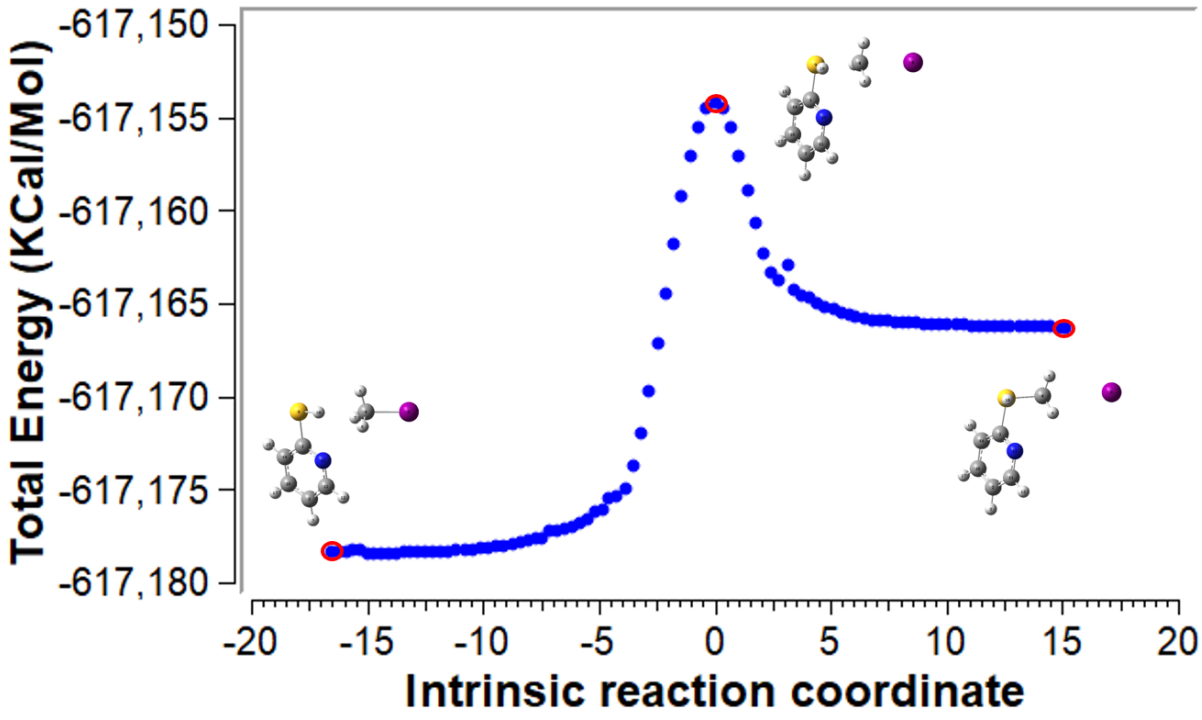

Figure S6. Full IRC calculations from the transition state of **13'**.

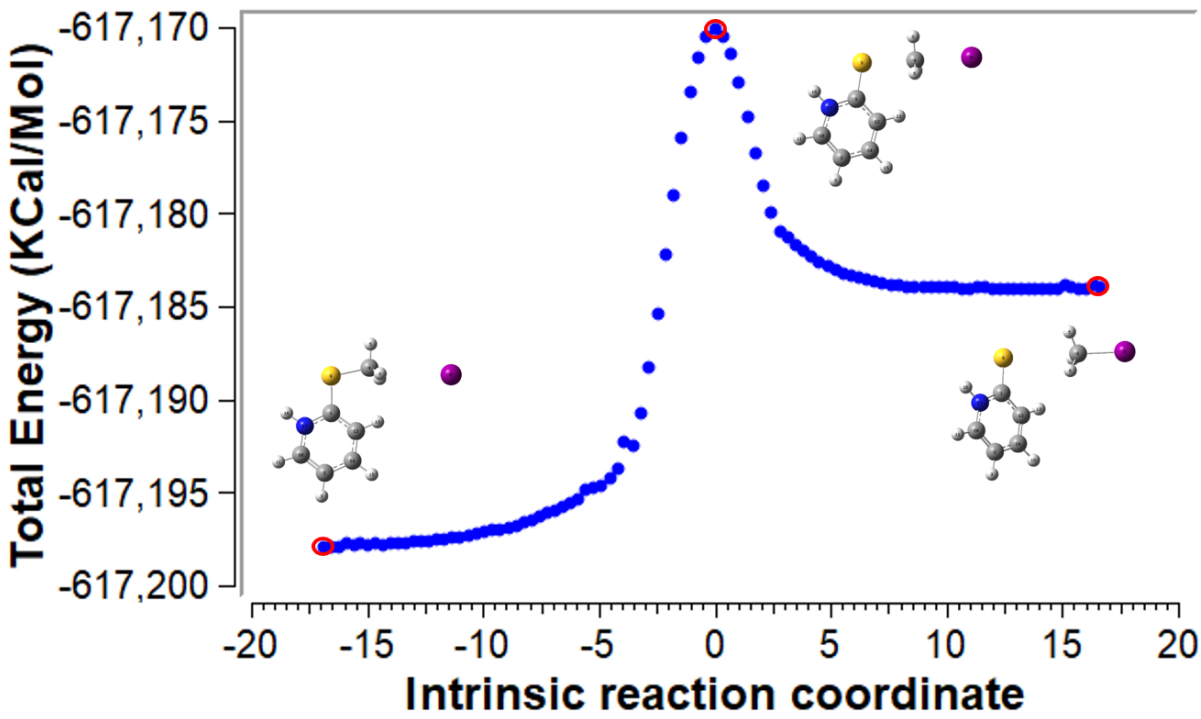

Figure S7. Full IRC calculations from the transition state of **13''**.

7. NMR characterizations (^{1}H and ^{13}C)

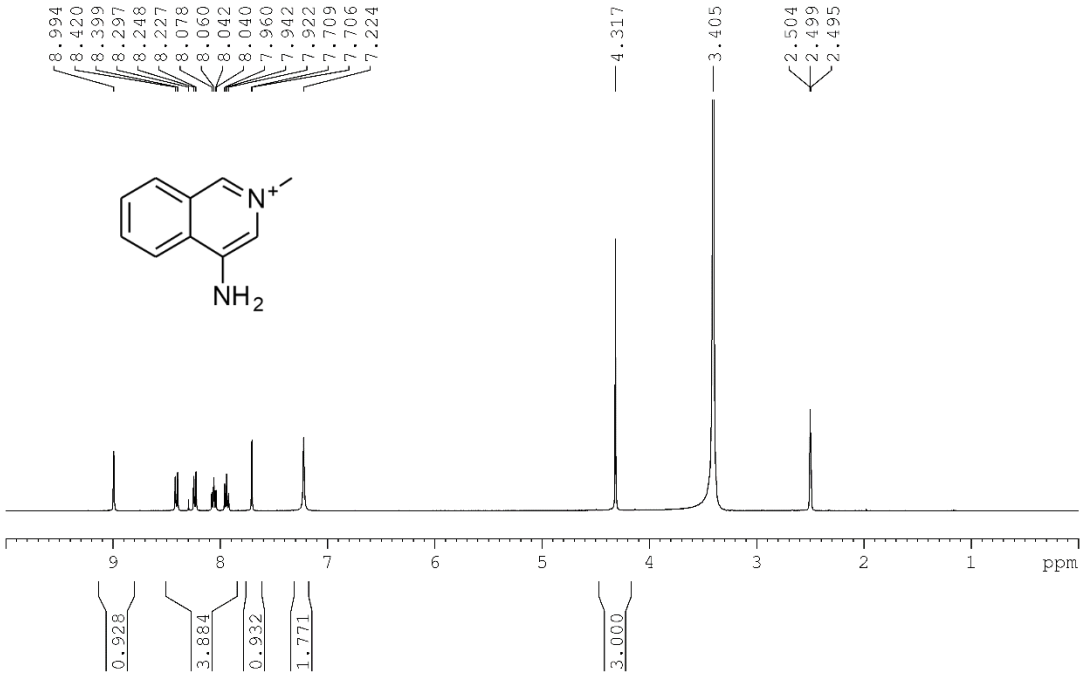

Figure S8. ^{1}H NMR of compound **1** in DMSO-d_6.

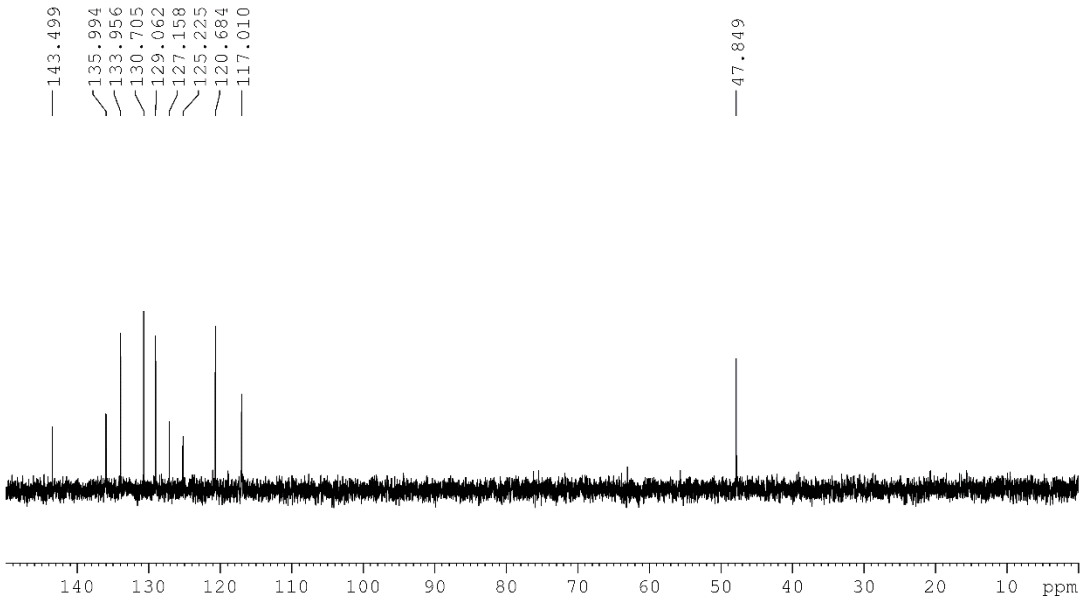

Figure S9. ^{13}C NMR of compound **1** in DMSO-d_6.

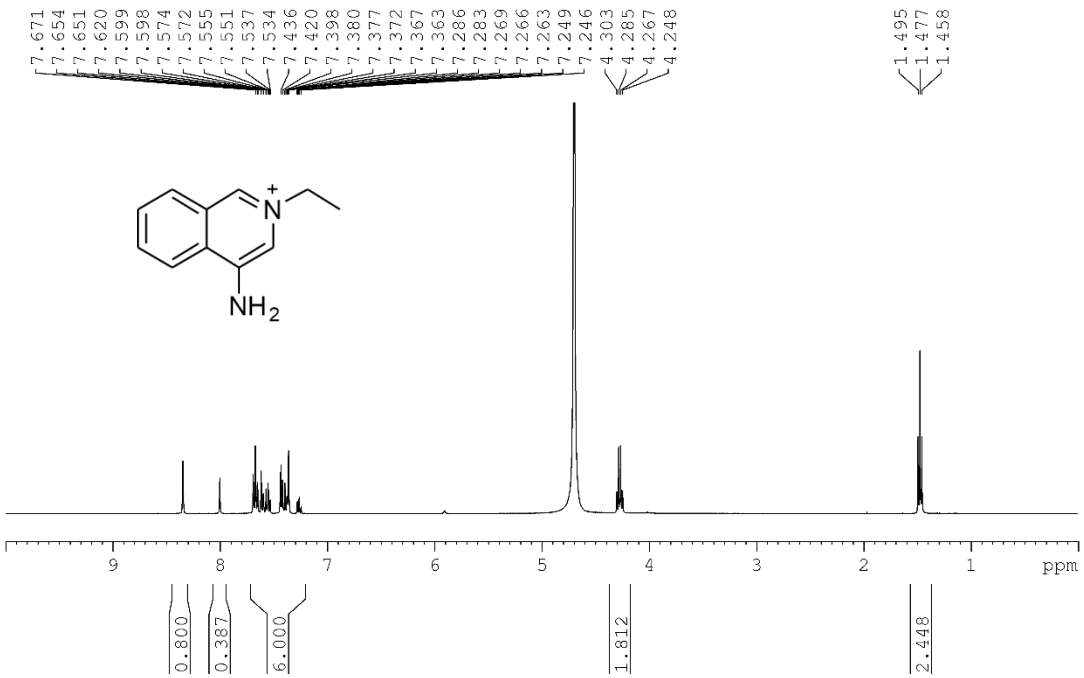

Figure S10. ^{1}H NMR of compound **2** in D_2O.

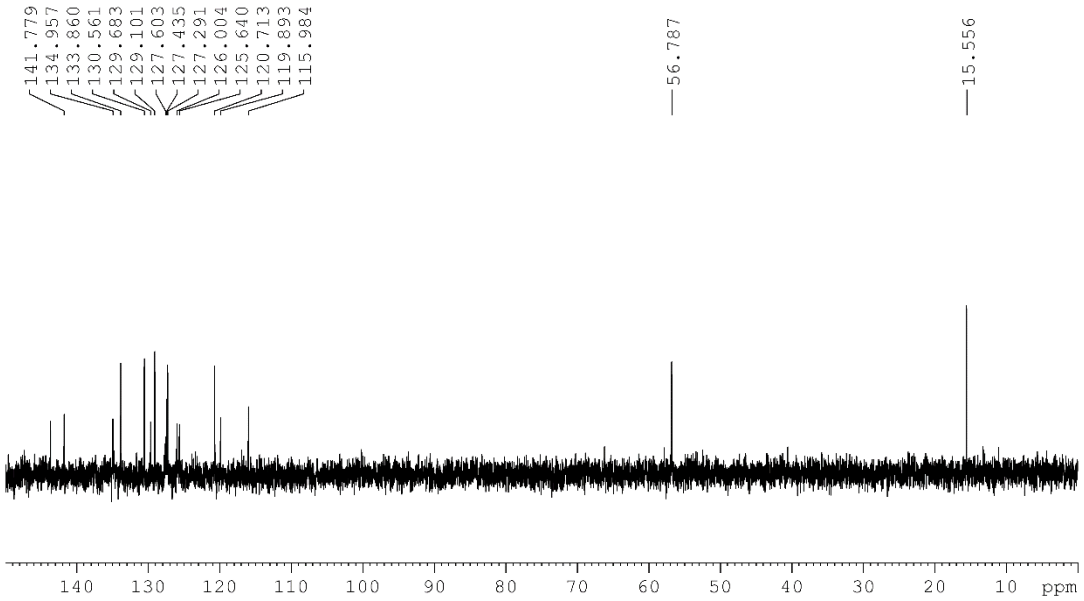

Figure S11. ^{13}C NMR of compound **2** in D_2O.

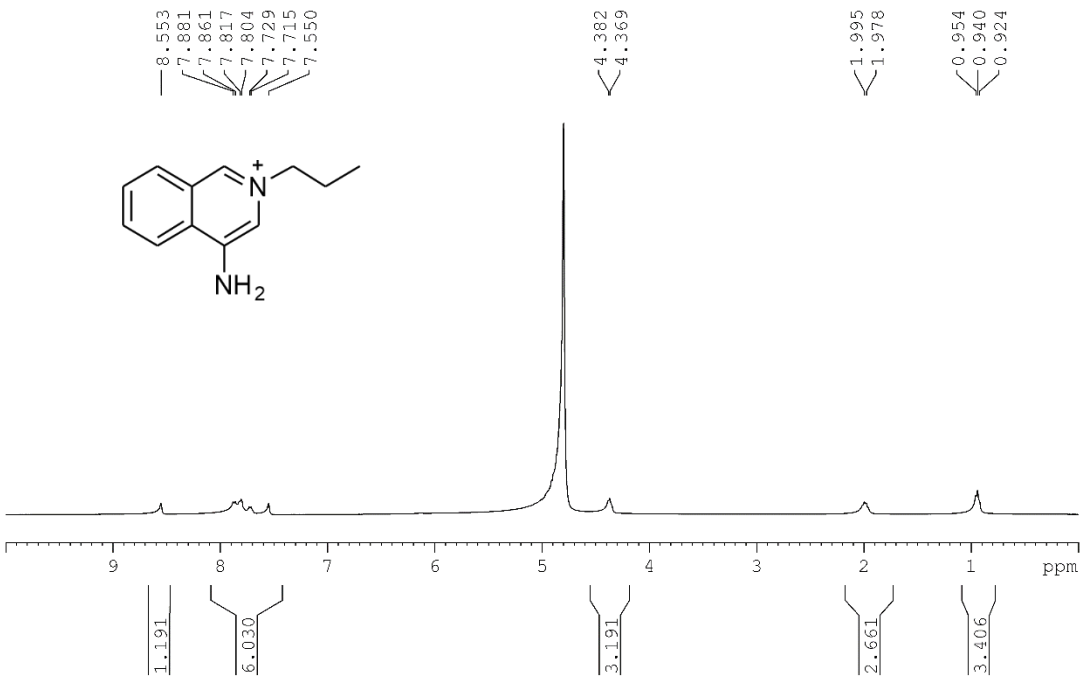

Figure S12. ^{1}H NMR of compound **3** in D_2O.

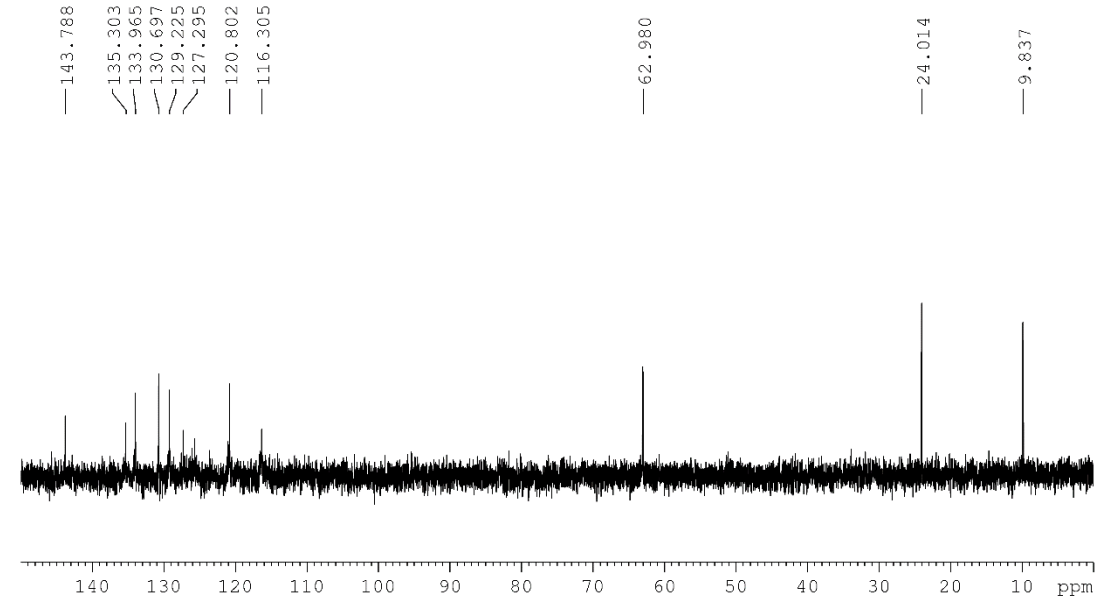

Figure S13. ^{13}C NMR of compound **3** in D_2O.

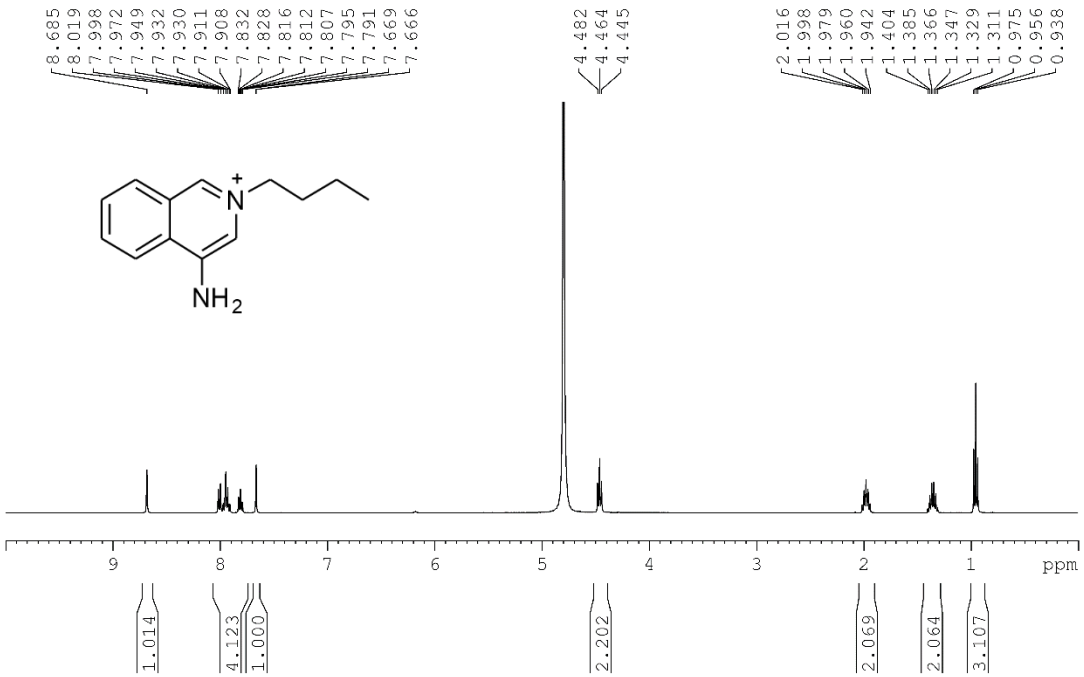

Figure S14. ^{1}H NMR of compound **4** in D_2O.

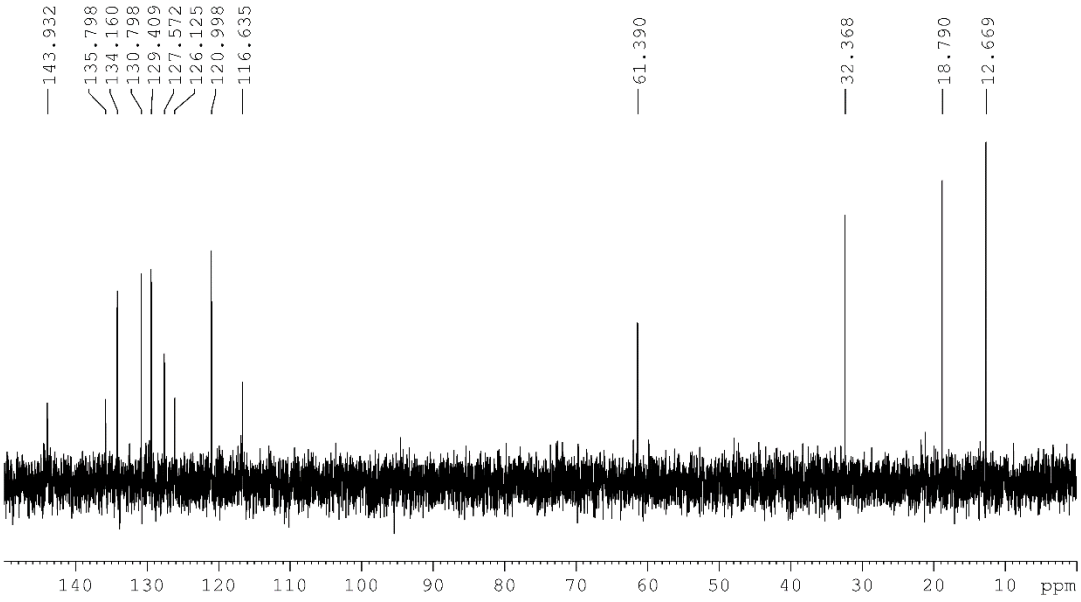

Figure S15. ^{13}C NMR of compound **4** in D_2O.

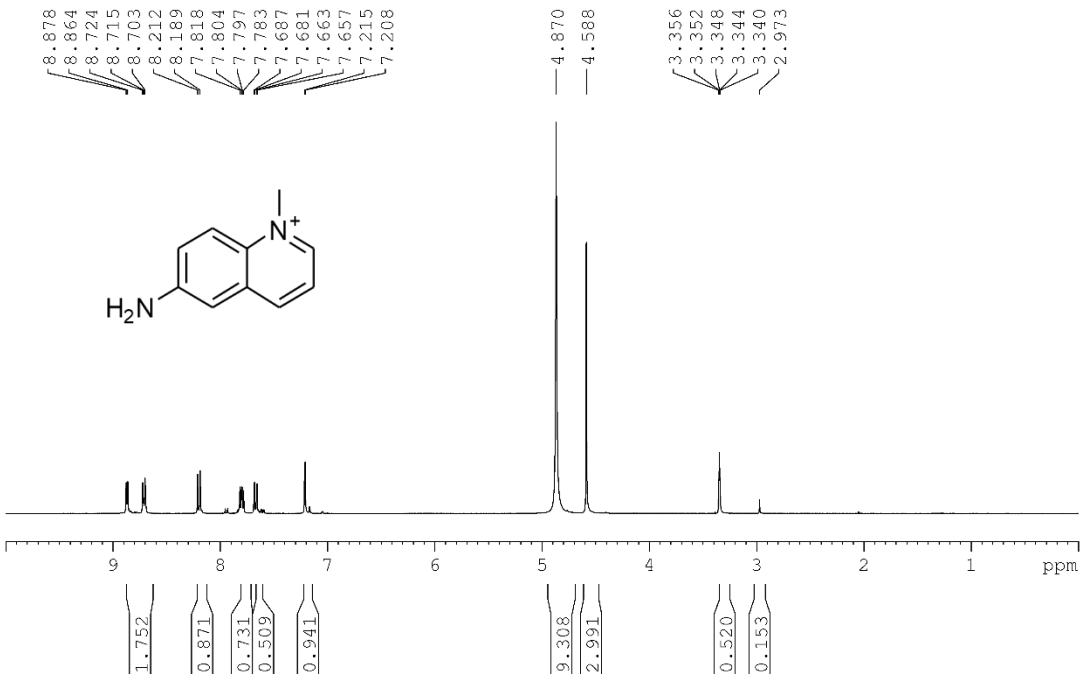

Figure S16. ^{1}H NMR of compound **5** in MeOH-d_4.

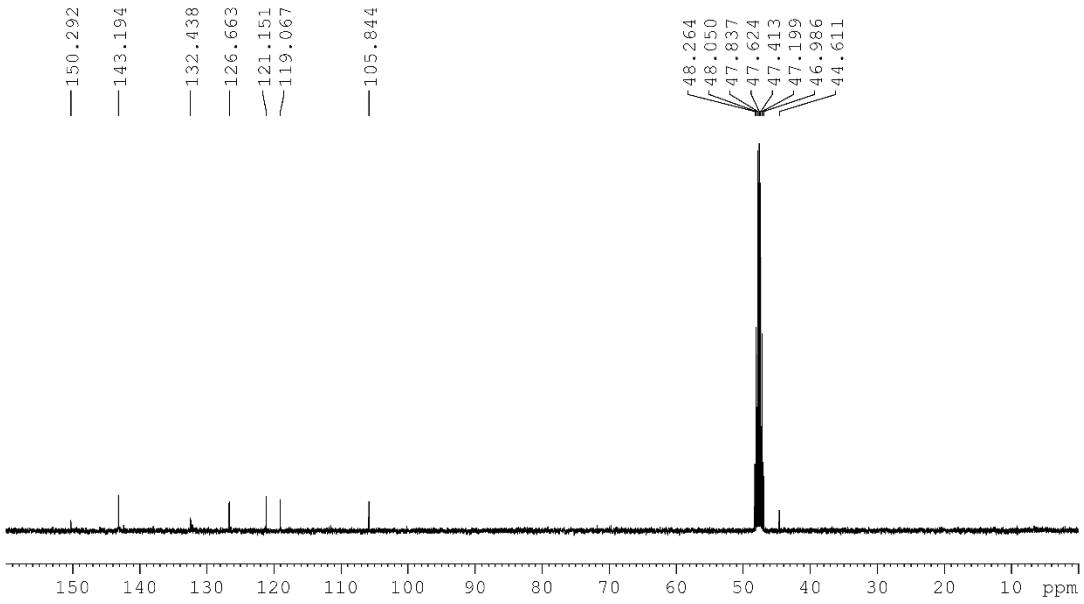

Figure S17. ^{13}C NMR of compound **5** in MeOH-d_4.

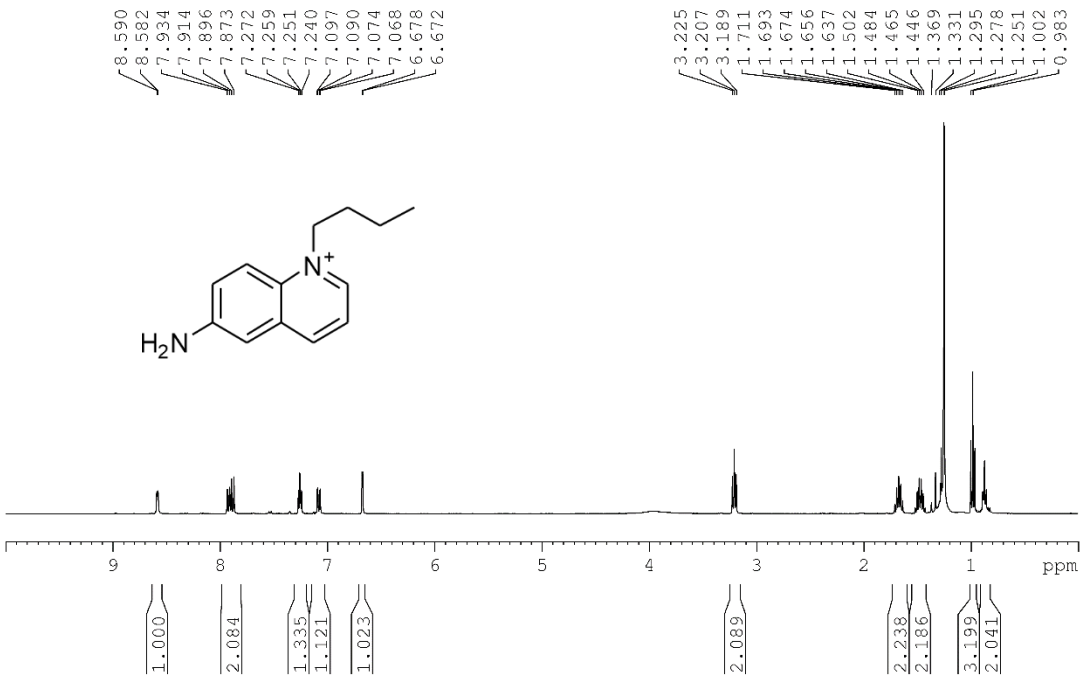

Figure S18. ^{1}H NMR of compound **6** in $CDCl_3$.

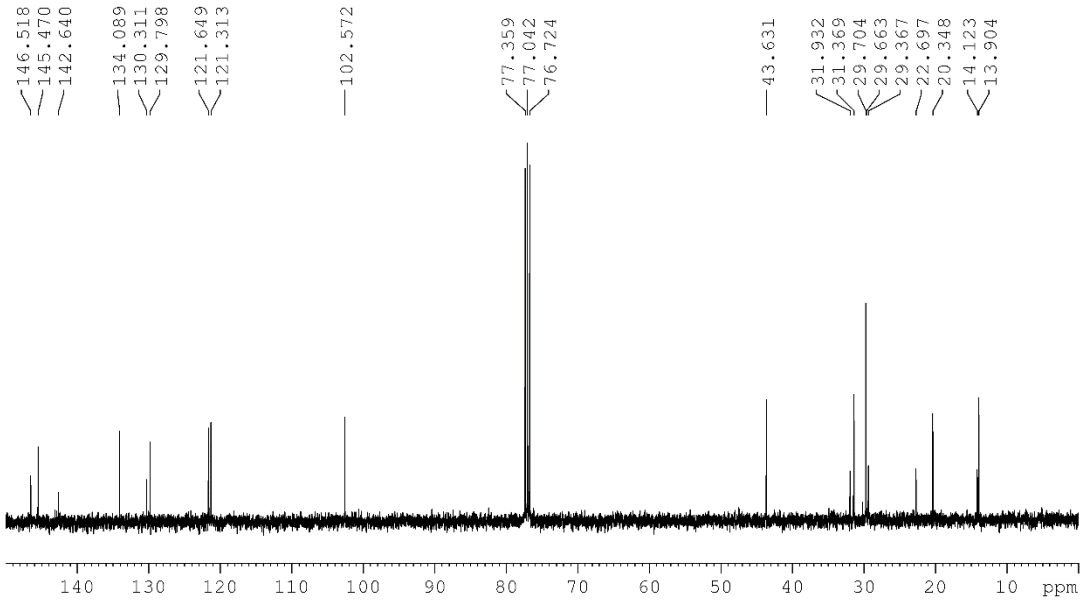

Figure S19. ^{13}C NMR of compound **6** in $CDCl_3$.

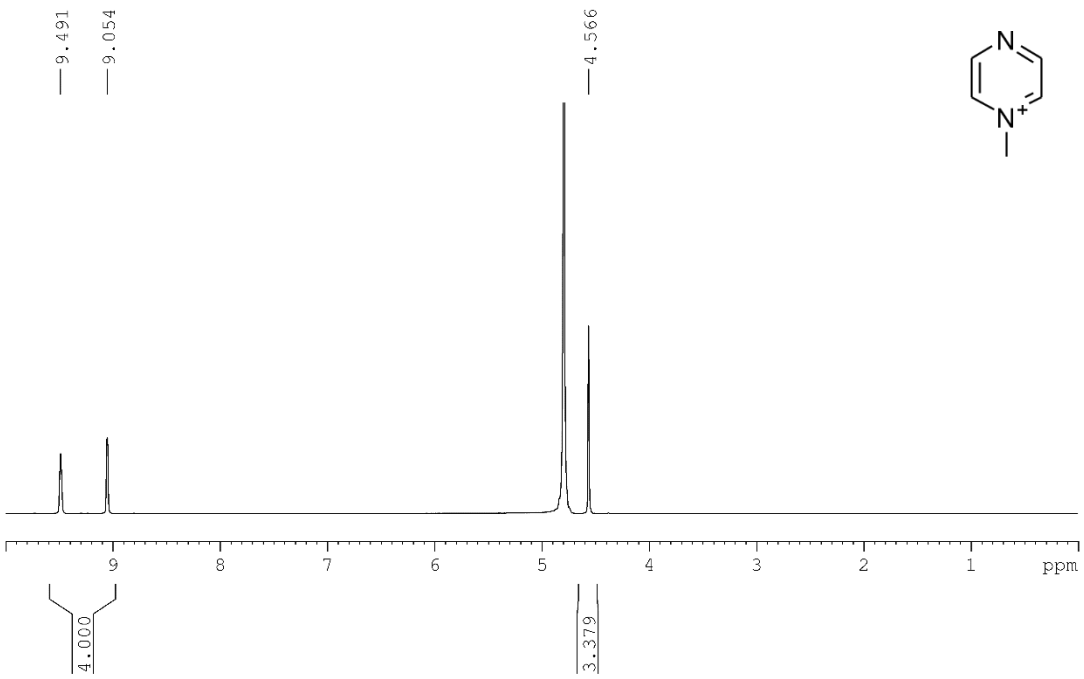

Figure S20. ^{1}H NMR of compound **7** in DMSO-d_6.

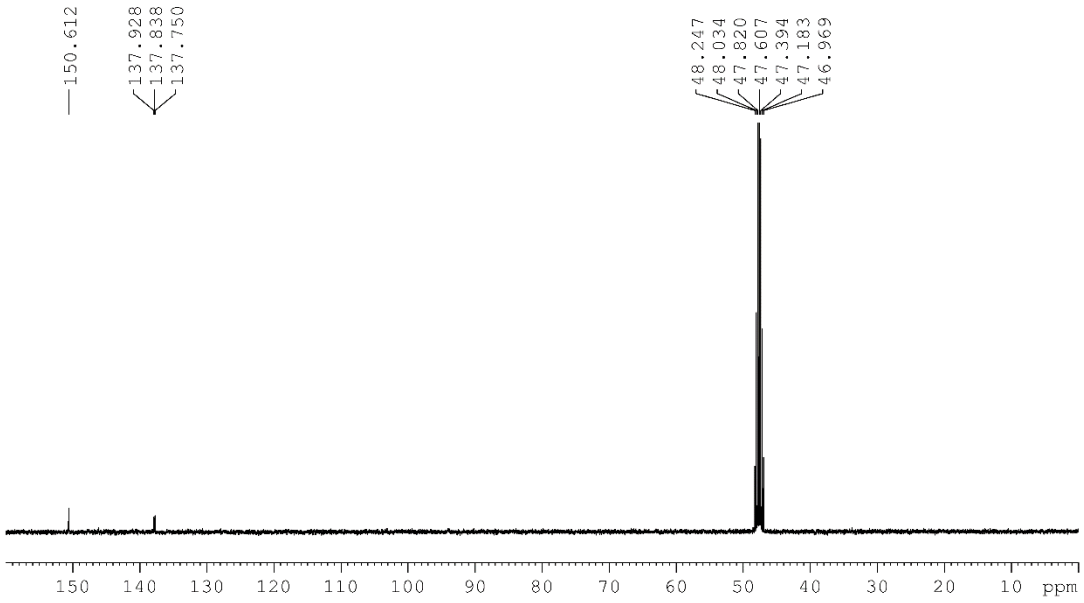

Figure S21. ^{13}C NMR of compound **7** in DMSO-d_6.

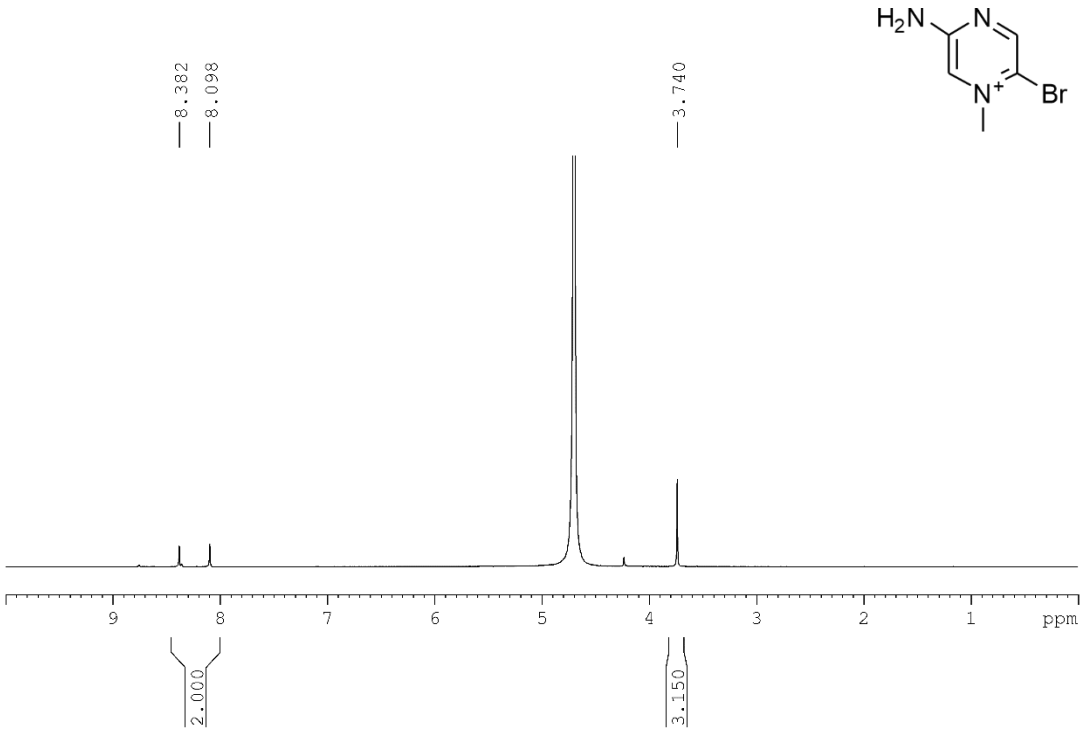

Figure S22. ^{1}H NMR of compound **8** in DMSO-d_6.

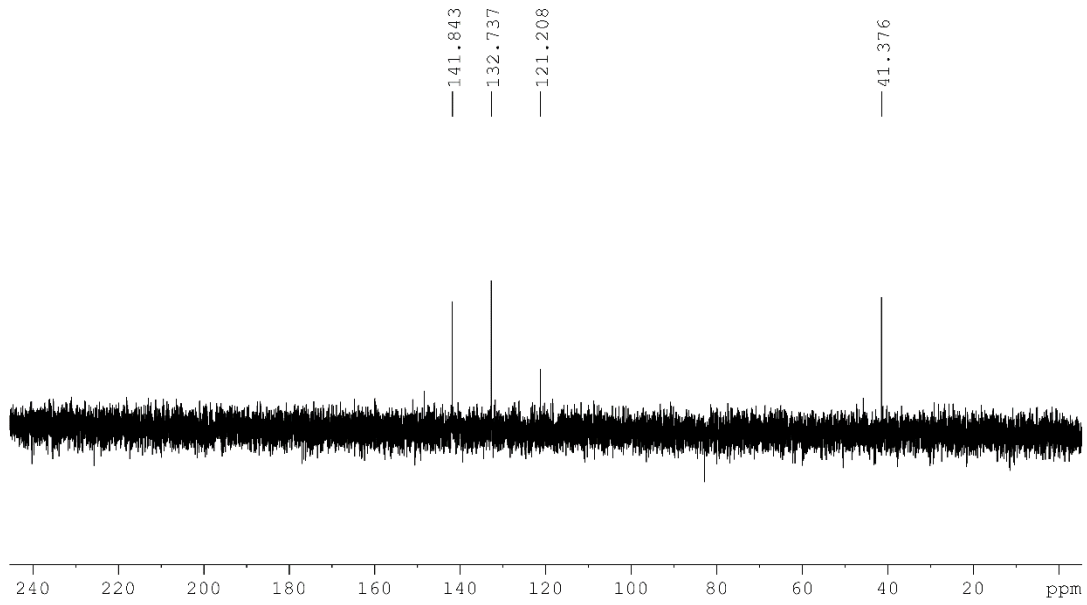

Figure S23. ^{13}C NMR of compound **8** in DMSO-d_6.

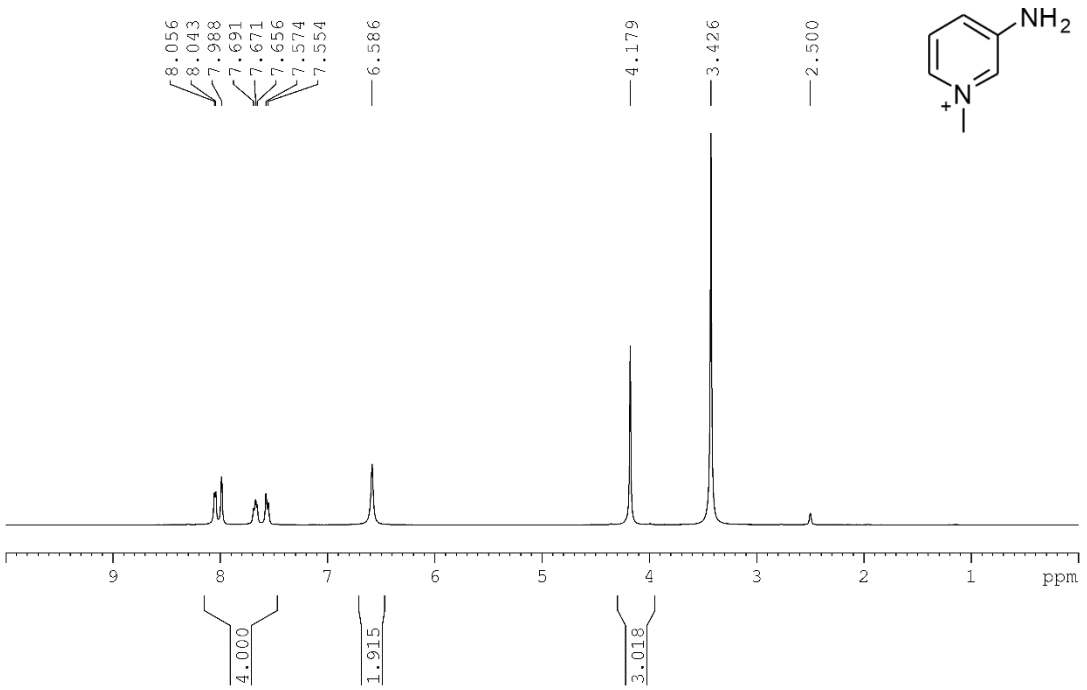

Figure S24. ^{1}H NMR of compound **9** in DMSO-d_6.

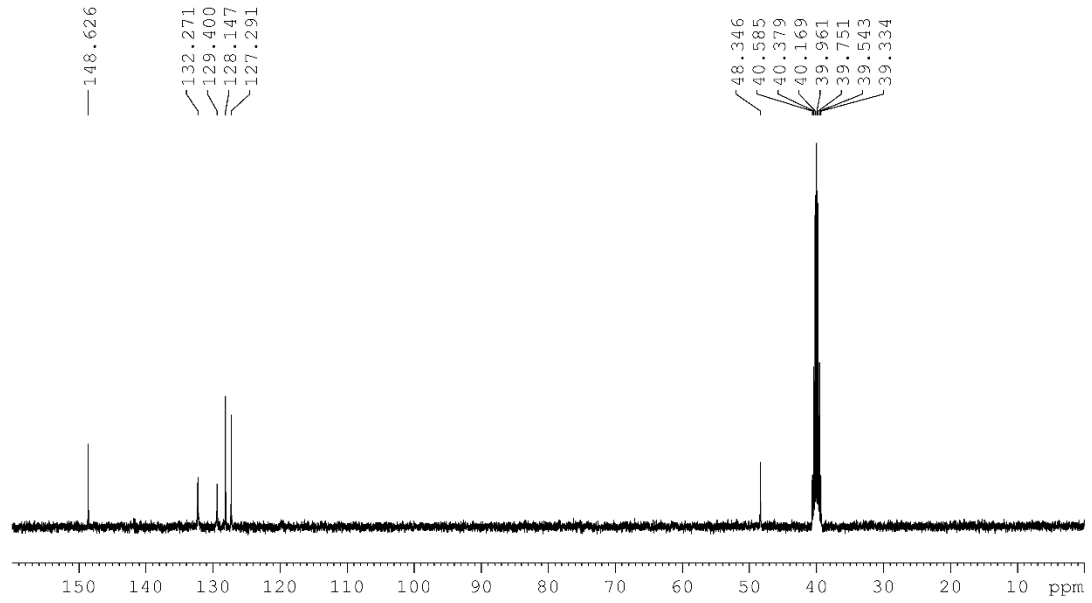

Figure S25. ^{13}C NMR of compound **9** in DMSO-d_6.

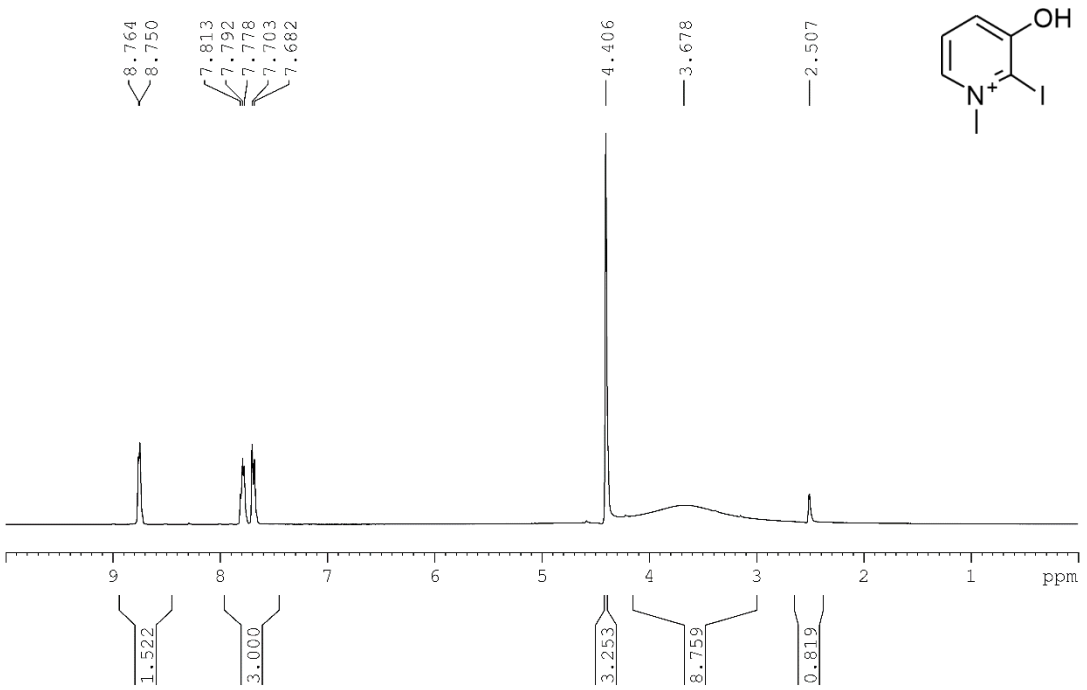

Figure S26. ^{1}H NMR of compound **10** in DMSO-d_6.

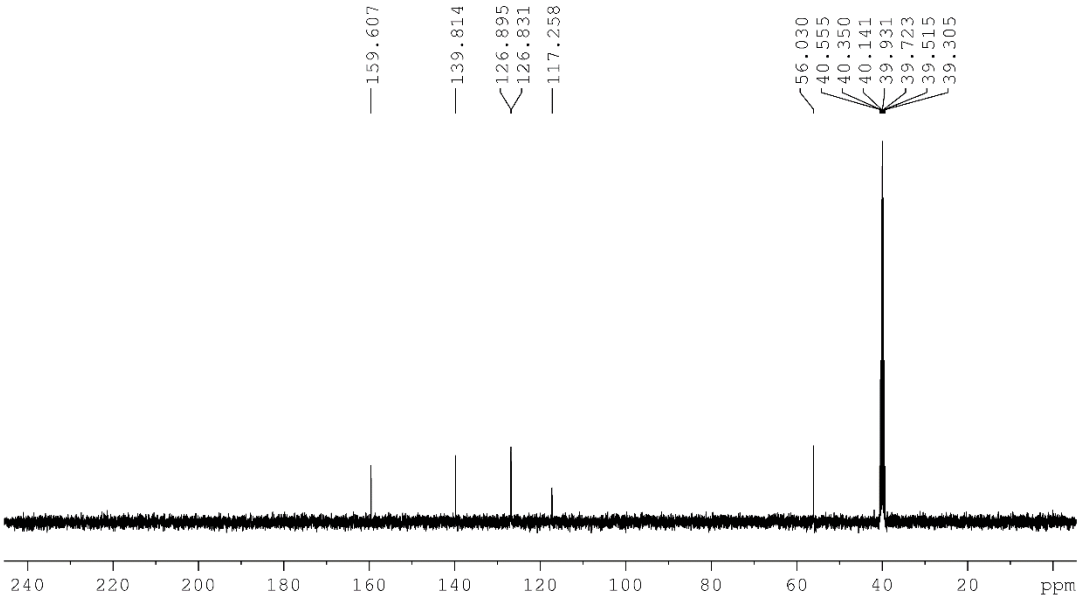

Figure S27. ^{13}C NMR of compound **10** in DMSO-d_6.

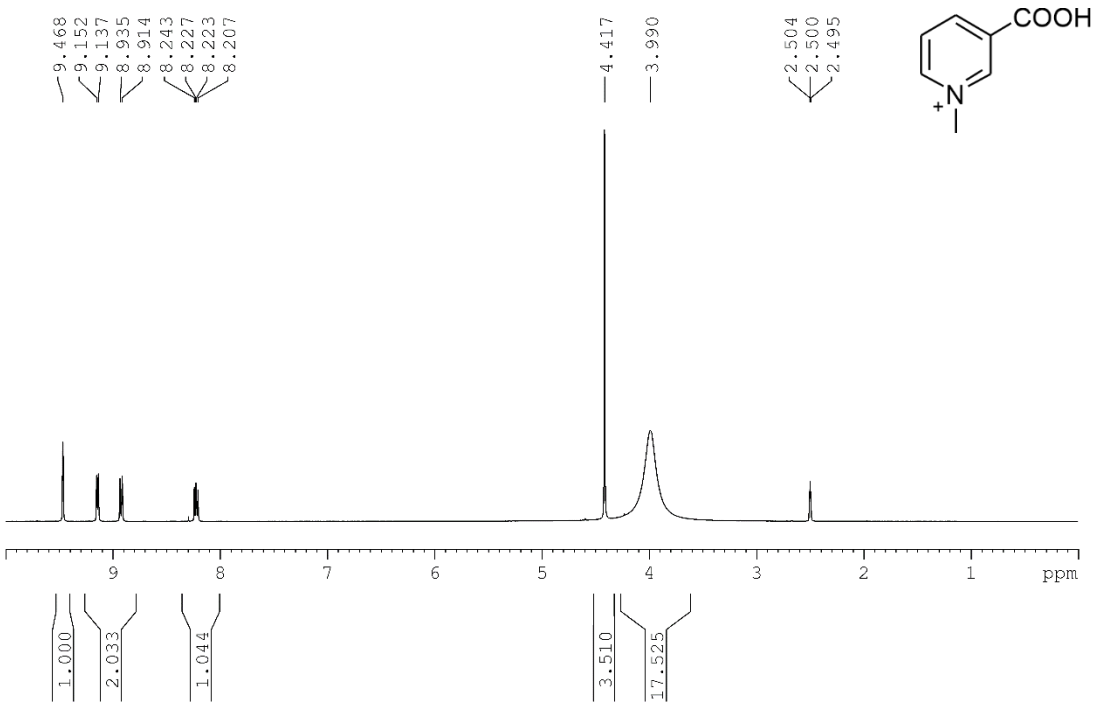

Figure S28. ^{1}H NMR of compound **11** in DMSO-d_6.

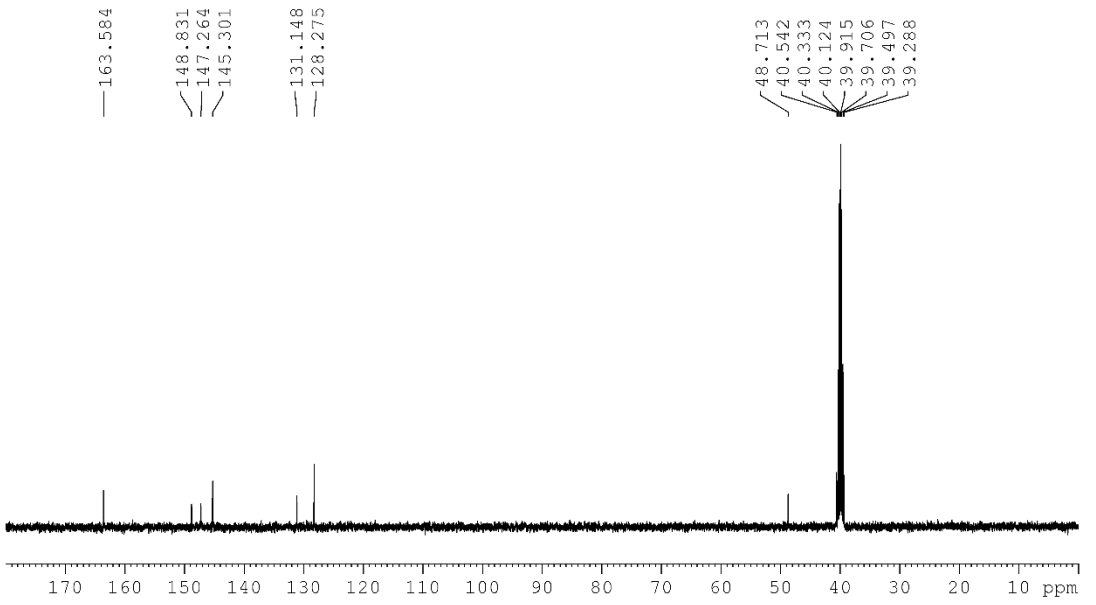

Figure S29. ^{13}C NMR of compound **11** in DMSO-d_6.

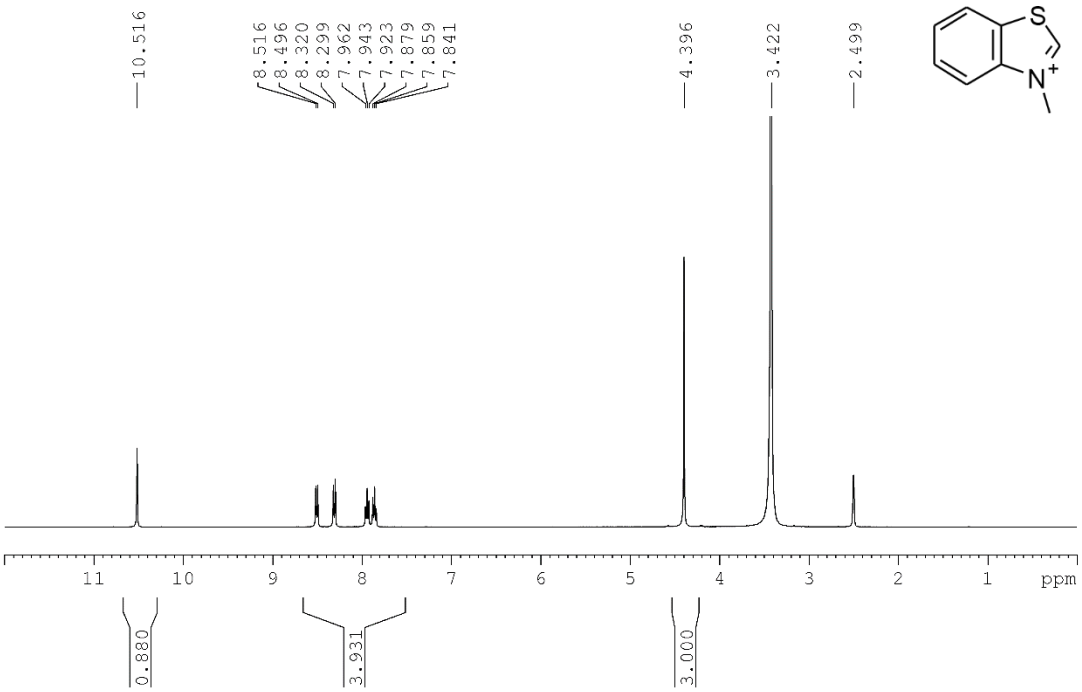

Figure S30. ^{1}H NMR of compound **12** in DMSO-d_6.

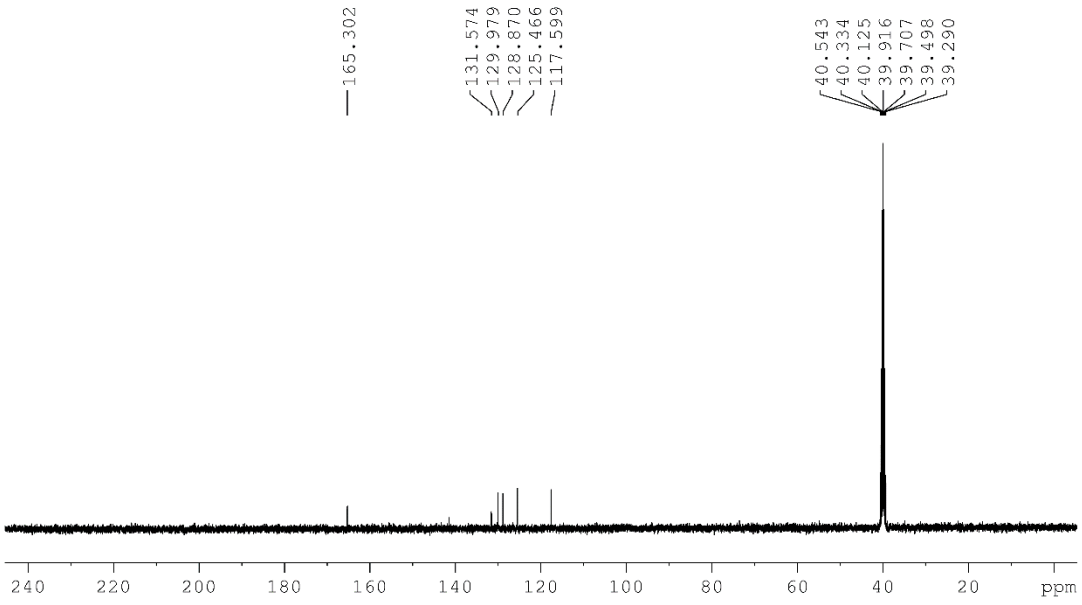

Figure S31. ^{13}C NMR of compound **12** in DMSO-d_6.

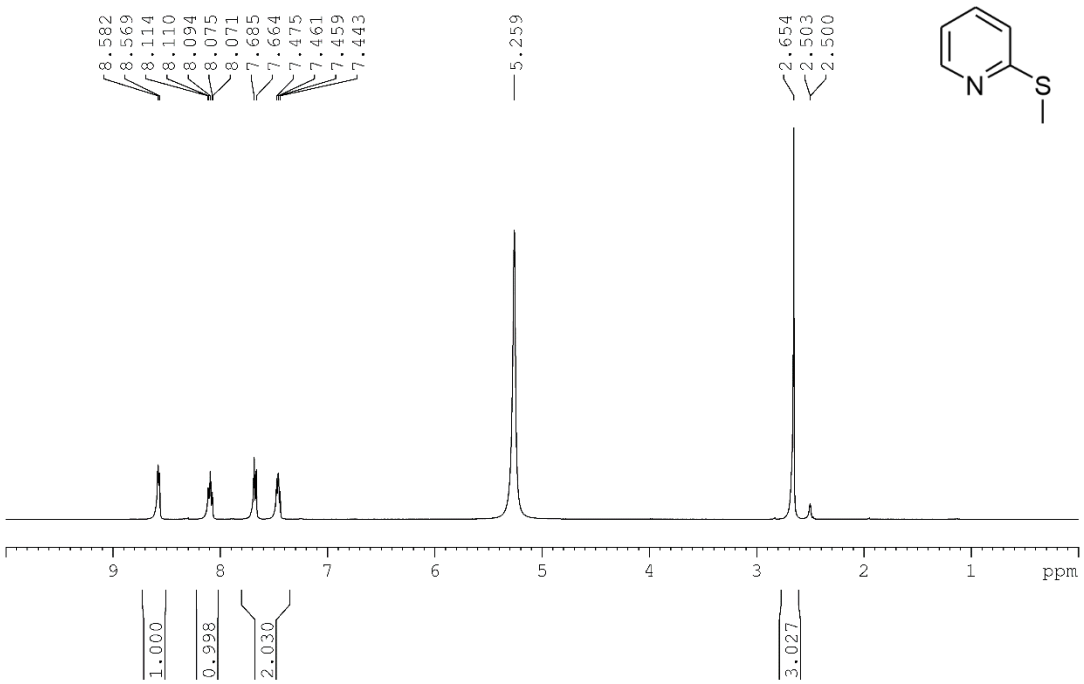

Figure S32. ^{1}H NMR of compound **13”** in DMSO-d_6.

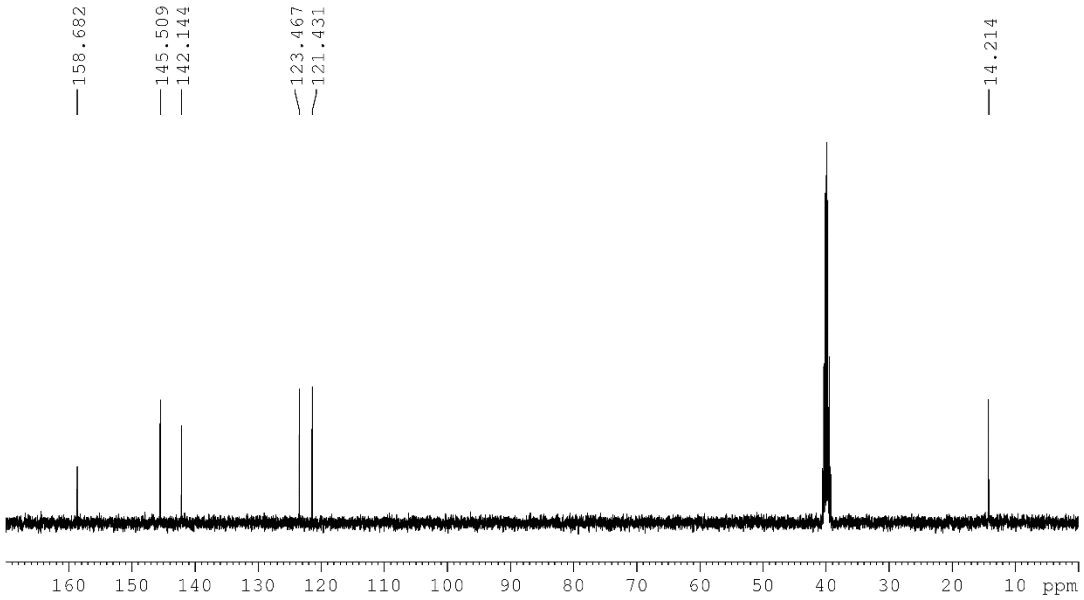

Figure S33. ^{13}C NMR of compound **13”** in DMSO-d_6.

8. References

1. Frisch, M. J.; Trucks, G. W.; Schlegel, H. B.; Scuseria, G. E.; Robb, M. A.; Cheeseman, J. R.; Scalmani, G.; Barone, V.; Petersson, G. A.; Nakatsuji, H.; Li, X.; Caricato, M.; Marenich, A. V.; Bloino, J.; Janesko, B. G.; Gomperts, R.; Mennucci, B.; Hratchian, H. P.; Ortiz, J. V.; Izmaylov, A. F.; Sonnenberg, J. L.; Williams; Ding, F.; Lipparini, F.; Egidi, F.; Goings, J.; Peng, B.; Petrone, A.; Henderson, T.; Ranasinghe, D.; Zakrzewski, V. G.; Gao, J.; Rega, N.; Zheng, G.; Liang, W.; Hada, M.; Ehara, M.; Toyota, K.; Fukuda, R.; Hasegawa, J.; Ishida, M.; Nakajima, T.; Honda, Y.; Kitao, O.; Nakai, H.; Vreven, T.; Throssell, K.; Montgomery Jr., J. A.; Peralta, J. E.; Ogliaro, F.; Bearpark, M. J.; Heyd, J. J.; Brothers, E. N.; Kudin, K. N.; Staroverov, V. N.; Keith, T. A.; Kobayashi, R.; Normand, J.; Raghavachari, K.; Rendell, A. P.; Burant, J. C.; Iyengar, S. S.; Tomasi, J.; Cossi, M.; Millam, J. M.; Klene, M.; Adamo, C.; Cammi, R.; Ochterski, J. W.; Martin, R. L.; Morokuma, K.; Farkas, O.; Foresman, J. B.; Fox, D. J. *Gaussian* 16, Wallingford, CT, 2016.

2. Marenich, A. V.; Cramer, C. J.; Truhlar, D. G., Universal solvation model based on solute electron density and on a continuum model of the solvent defined by the bulk dielectric constant and atomic surface tensions. *J. Phys. Chem. B* 2009**,** 113 (18), 6378-6396.